Numerical Methods in Civil Engineering, 8-2 (2023) 80-91

Numerical Methods in Civil Engineering

Journal Homepage: https://nmce.kntu.ac.ir/

Application of the material point method in the modeling of arching effects behind retaining walls with active movements

Akbar Rouzkhosh[*], Siamak Zadkarim[**], Masoud Pourbaba[*]

ARTICLE INFO

RESEARCH PAPER

Article history:
Received:
May 2023
Revised:
October 2023
Accepted:
January 2024

Keywords:
Arching effect;
Material point method;
Finite element method;
Retaining wall;
Active movement;
Physical modeling.

Abstract:

Numerical modeling of problems with large deformations is one of the main challenges in computational mechanics. Conventional numerical approaches cannot accurately model large deformations. Recently, the material point method (MPM), which comprises advantages of Eulerian and Lagrangian descriptions of movement, has been developed to solve complicated numerical problems such as large deformations. In this paper, the MPM method is employed to model the behavior of a soil mass behind a rigid retaining wall during active movement. It is the first time that the accuracy of the MPM method has been evaluated in the modeling of retaining walls with active movements. The accuracy and efficiency of the MPM are measured using two small-scale physical modeling tests and an analytical approach (for translational motion). In addition, a comparison between the results of the MPM and conventional FEM is provided. It is shown that the MPM can model the arching effect in the soil media better than the FEM; however, the material point method leads to smaller stresses on the wall compared to experimental results. It is demonstrated that the employed MPM can accurately model arching effects on the soil media behind the retaining walls with active movement. For transitional movement, arching effects lead to the upward movement of the resultant horizontal force on the wall, which occurs higher than 1/3H (H is the height of the wall). The achieved results indicate that the traditional methods can lead to overestimated designs without considering arching effects.

Nomenclature

Dr	Relative density
τ	Shear stress
σ'	Effective stress
L	Length
D	Width
E	Elastic modulus
u	Displacement
v	Velocity
m	Mass of each material point
M	Lumped mass matrix
p	Momentum vector
a	Acceleration

* *Department of Civil Engineering, Maragheh Branch, Islamic Azad University, Maragheh, Iran.*
** *Corresponding author: Department of Civil Engineering, Bonab Branch, Islamic Azad University, Bonab, Iran. Email: S_Zadkarim@Yahoo.Com*

1. Introduction

Determination of the soil lateral pressure on the retaining walls is one of the classical problems in soil mechanics. Coulomb and Rankine's theories, which have been developed based on the limit equilibrium method, have comprehensively been applied to calculate lateral soil pressures. The Rankine theory neglects the roughness and slope of the walls, and the Coulomb theory is not capable of considering the pattern of the stress distribution behind the wall (Terzaghi, 1943 [1]). Based on the Rankine theory, lateral soil pressure increases linearly by increasing the depth of the soil media.

The experimental studies have revealed that the lateral soil pressure behind the rigid retaining walls with transitional or rotational movements will be nonlinear because of the arching effects in the soil mass. The arching effect in the soil media can be defined as transmitting some parts of the soil pressures from an unstable soil wedge to a stable part of the

https://doi.org/10.61186/NMCE.2303.1021

soil mass; therefore, less pressure will be tolerated with retaining walls (Patel & Deb, 2020 [2]).

In addition to the retaining walls, arching is a common phenomenon in buried geotechnical structures such as tunnels and group piles (Abbasnezhad & Sadrekarimi, 2008 [3], Li, 2018 [4]; Zhang et al., 2022 [5]). Redistribution of the soil pressure induced by arching effects can influence the tolerated forces in adjacent structures. Therefore, ignoring the arching effects can make the design of geotechnical projects conservative and expansive. In addition, arching effects in the soil mass behind the retaining walls can affect the location of the resultant lateral forces and, hence, can induce mistakes in the calculation of the stability of these structures (for example, in the calculation of the factor of safety against overturning). Janssen (1895) [6] proposed the arching theory based on the pressure of the granular materials in the silos. Terzaghi (1943) [1] showed that the maximum lateral earth pressure does not occur at the bottom of the retaining walls. In this study, Terzaghi (1943) [1] defined arching as the capability of transmitting shear stresses from a part of the soil mass to a more stable part of the soil. Frydman and Keissar (1987) [8] studied the distribution of stresses behind the rigid walls under active and in rest situations by applying some centrifuge experiments. This study contains only rotational movement of the rigid wall. It has been shown that the lateral soil pressure on the wall has a nonlinear distribution. In addition, it has been demonstrated that the resultant lateral force acts higher than the one-third height of the bottom of the wall. Chenghua et al. (2001) [9] proposed an analytical approach to calculate lateral pressure on retaining walls. It was assumed that the resultant lateral force would be equal to the resultant force proposed by Coulomb. Paik and Salgado (2003) [10] proposed an analytical approach to determine the lateral pressure of soil media on retaining walls by considering the distribution of lateral stresses corresponding to a wedge of a circle (because of the arching effects). However, such a distribution of stresses is not true for soil mass; the simplicity of the relationships can be remained by such an assumption. Handy and Spangler (2007) [11] proposed an analytical method to calculate active earth pressure by considering the effects of arching. It was indicated that the linear distribution of lateral soil pressures is not true, but the assumption of the linear distribution will not result in significant errors in the design. Goel and Patra (2008) [12] considered both translational and rotational rigid movements of retaining walls to extract an analytical solution to calculate lateral soil pressures in the presence of arching effects. It was shown that the shape of the failure surface not only depends on the amount of movement but also depends on the interfacial friction between the wall and soil media. Different researchers proposed other analytical approaches to determine lateral soil pressures by considering the effects of the arching based on the aforementioned methods (Pipatpongsa and Heng, 2010 [13], Dalvi & Pise, 2012 [14]). Various studies have been done to evaluate the effects of different parameters on the behavior of retaining walls and the soil media behind them. Bahmani Tajani et al. (2022), Deng and Yang (2019) [15], Fathipour et al. (2022) [16], Fathipour et al. (2021)[17], Shahrokhabadi et al. (2019) [18], Liang et al. (2012)[19], Stanier and Tarantino (2010) [20], and Sahoo and Ganesh (2017) [21], and Pufahl et al. (1983) [22] investigated of the behavior od retaining walls against horizontal pressure of unsaturated soils. In addition to different saturation conditions of the soil media, some other investigations have been applied using numerical methods to evaluate effective parameters on the behavior of (Veiskarami et al. 2023 [23], Mirmoazen et al. 2022 [24], Payan et al. 2022 [25], Mirmoazen et al. 2021 [26], Vahedifard et al. 2015 [27], Patki et al. 2015 [28], Vo and Russell 2014 [29], Zhang et al. 2012 [30], Farajniya et al. 2022 [31], Zhao et al. 2009 [32], Soubra 2000 [33]). Besides the static behavior, the seismic behavior of retaining walls attracted lots of investigations, as well (Fathipour et al. 2021 [34, 35], Li et al. 2010 [36], Aalami et al. 2022 [37], Veiskarami et al. 2019 [38]). Conventional numerical approaches that have been developed based on the principles of the continuum mechanics, such as the finite element method (FEM), the finite differences method (FDM), and the boundary element method (BEM), were undertaken to model retaining walls in different studies (Nakai, 1985 [39], Dasgupta et al. 2017 [40], Hajialilue-Bonab and Tohidvand 2015 [41], Hassanzadeh et al. 2018 [42], and Morgan et al. 2013 [43]). These methods have some drawbacks that make them unsuitable for modeling some complicated geotechnical problems. For example, in problems with large deformations, mesh distortion can lead to inaccurate results. However, the conventional continuum mechanics method like the FEM or the FDM can be modified (for example, by using geometrical nonlinearity) to model large deformations; there are several issues in using such a modified method as follows:

- The geometrical nonlinear method can be more computationally expensive compared to conventional numerical methods like the FEM and the FDM.
- The geometrical nonlinear method can lead to singularity in the stiffness matrix, which can cause numerical issues in calculations.
- Application of geometrical nonlinearity can reduce the results of the material nonlinearity in the FEM or the FDM.

Dealing with contacts in these methods also is not straightforward. Harlow (1964) [44] proposed a method, which was named the particle-in-cell method (PIC), to model the flow of fluids. Sulsky and Schreyer (1994) [45]

developed this particle-based method using the discretization of the dynamic momentum equilibrium equation for solid materials. By modifying, extending, and developing the PIC method, a relatively novel approach was proposed that is named the material point method (MPM) these days. The main feature of the MPM is related to its formulation, which employs both Lagrangian and Eulerian descriptions of movement. Such a coupled Lagrangian-Eulerian numerical approach can solve inherent problems of the mesh-based approach like the conventional FEM. In addition, dealing with multi-phase materials, contact problems, and large deformations can be done using MPM without extra effort based on its original formulation. A detailed description of the equations of the MPM method is presented in Section 2 of this paper. Different researchers used the MPM method to solve various geotechnical problems. Higo et al. (2010) [46] used a three-phase MPM approach to study the mechanical behavior of unsaturated soils. Wang et al. (2015) [47] the MPM method based on the implicit formulation to make the application of the advanced constitutive models easier. In the proposed implicit formulation, there is not any restriction on the selection of time steps, as well. Ceccato (2015) [48] used the MPM to model a cone penetration problem, and it was shown that the MPM could accurately model the deal large deformation problem. Bolognin et al. (2017) [49] applied the MPM approach to model the fluidization of a sandstone. Kiriyama et al. (2018) [50] modeled the seismically induced liquefaction of sands by the MPM using a two-phase modeling approach. Giridharan et al. (2020) [51] developed a hypoplastic constitutive model consistent with the MPM formulation to model liquefaction of sands and compared the results of the model with Hypoplastic constitutive relations with the model with the UBCsand constitutive relations.

However, the material point method has been used to model different geotechnical problems; there is not any study about the accuracy and efficiency of this method in the simulation of arching effects behind retaining walls. It has been revealed by various studies that the traditional methods for estimating of the earth pressure on creating walls could result in estimation designs. Therefore, the MPM as a capable method for large deformations could be considered as a potentially efficient method for these problems. The MPM could be used for any boundary value problem, including passive retaining wall movement. However, MPM is mostly efficient for calculating displacements rather than stresses. In this paper, for the first time in the literature, the MPM is used to model an active retaining wall. The one-phase formulation is undertaken as the selected soils are dry, and the classic Mohr-Coulomb constitutive model is used for stress-strain relationships. The accuracy of the results is compared with some analytical methods and experimental approaches, and the feasibility of the MPM method in the modeling of retaining walls is discussed. The accuracy of the results of the employed MPM method in considering arching effects is studied, as well. The main aim of this study is the evaluation of the efficiency and accuracy of the MPM method in the modeling of active movement of the retaining walls, including arching effects. As described in the paper, arching effects can result in a reduction in the applied stresses on the retaining wall. Therefore, traditional methods like Coulomb or Rnkin methods can lead to overestimated designs. Based on this description, the application of the MPM method to the modeling of arching effects on the earth-induced loads on the wall is discussed in the paper.

2. Numerical and experimental methods

2.1 Employed numerical approach

To describe movement in material, there are two main numerical approaches. In the first one, which is named the Eulerian description of movement, governing differential equations are solved in a constant computational mesh. The material can move through such a constant mesh; therefore, the history of deformation for a certain particle cannot be tracked in this approach. In the second approach, which is called the Lagrangian method, the computational mesh is attached to the material, and this mesh would be deformed by the occurrence of deformation in the material. The main disadvantage of the Lagrangian description of movement is the mesh distortion in the problems with large deformations. However, such a mesh distortion will be avoided in the Eulerian description of movement; there are some drawbacks in the Eulerian approach that can be summarized as follows:

- Problems in the numerical modeling of material with history-dependent behavior like soils.
- Problems in the definition of boundary conditions.
- Dealing with some terms in differential equations makes solving them more complicated.

The material point method (MPM) has been developed to use the advantages of the Eulerian and Lagrangian description of movement. In this method, a constant computational mesh and material properties are carried out using some particles. The main differences between the MPM and FEM can be considered as the integration scheme of these methods. In the FEM, numerical integration is performed using Gauss points. In the MPM, numerical integration is done by using material points. As shown in Figure 1, material points can move from one element to another, whereas Gauss points have to remain inside the element throughout the analysis.

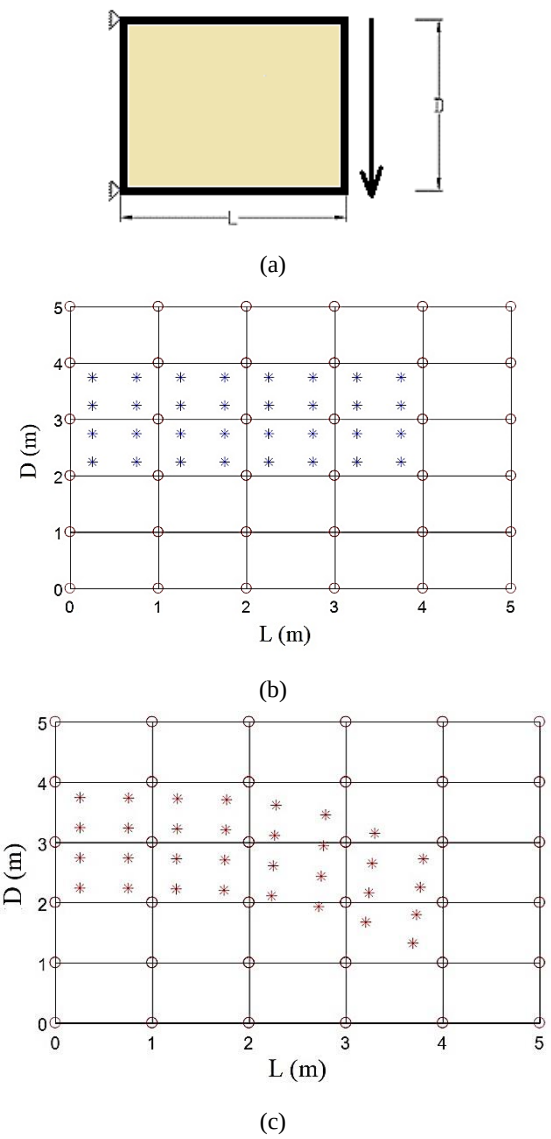

Fig. 1: An elastic beam under fixed static force at its end (b) computational mesh and material points before applying force (c) computational mesh and material points after applying force

Besides the great advantages of the MPM, this method has some disadvantages that can be summarized as follows:

- The MPM is more computationally expensive compared to the conventional FEM and FDM.
- The results of the MPM are more accurate in displacements compared to stresses.
- Applying boundary conditions in the conventional FEM and FDM is more accessible than the MPM.

The algorithm of the MPM can be summarized as follows:

Step 1. Construction of mass matrix, internal and external force vectors.

It should be mentioned that for simplicity, instead of the consistent mass matrix, the lumped mass matrix could be used in the MPM. In this approach, Eq. (1) and Eq. (2) can be used to determine the mass of each material point.

$$m_{MP} = \rho_{MP}\,\Omega_{MP} \tag{1}$$

$$M_{lumped} = \sum_{el=1}^{num,el} \sum_{i=1}^{no,el} \sum_{mp=1}^{mp,el} N^T(\xi_{MP})\, m_{MP} \tag{2}$$

In Eq. (1) m_{MP} is the mass of each material point, ρ_{MP} is the mass density of the material, and Ω_{MP} is the corresponding volume of the selected MP. In Eq. (2) num, el is the number of elements in the computational mesh, *no*, *el* is the number of nodes in the element i, and mp, el is the number of material points in the element i. In this equation, $N^T(\xi_{MP})$ is the shape function for the corresponding material point, where ξ_{MP} denotes the location of the material point in the local coordinates system.

Step 2. Solve momentum equilibrium equation to calculate nodal accelerations

In this step, Eq. (3) should be solved to determine nodal accelerations.

$$a_i^k = M_i^k (f^{ext} - f^{int}) \tag{3}$$

In this equation, i is the number of nodes in the computational mesh, and k is the corresponding time step.

Step 3. Calculate velocities of material points and update nodal momentums.

By calculating the nodal accelerations, using the explicit time integration approach and interpolation of the nodal accelerations in the material points, velocities at the MPs can be determined using Eq. (4).

$$v_{MP}^{k+1} = v_{MP}^k + \Delta t \sum_{i=1}^{num,nod} N_i{}^T(\xi_{MP})\, a_i{}^k \tag{4}$$

In Eq. (4), v is the velocity vector, and Δt is the time step. Now, nodal momentums can be calculated using Eq. (5). In this equation, p is the nodal momentum vector.

$$p_i^{k+1} = \sum_{el=1}^{num,el} \sum_{MP=1}^{num,MP} m_{MP} N_i{}^T(\xi_{MP})\, v_{MP}{}^{k+1} \tag{5}$$

Step 4. Update nodal velocities.

Using the nodal momentums, velocities of nodes in computational mesh for the current time step can be achieved by Eq. (6).

$$v_i^{k+1} = \frac{p_i^{k+1}}{M_i{}^k} \tag{6}$$

Step 5. Calculate increments of displacements in nodes. Increments of displacements can be calculated using nodal velocities by Eq. (7).

$$\Delta u_i^{k+1} = \Delta t\; v_i^{k+1} \tag{7}$$

Step 6. Calculate strain increments

Using the matrix of B (which contains differentials of shape functions with respect to spatial direction), which can be

determined in the same manner as the finite element method, increments of strains can be achieved as defined in Eq. (8).

$$\Delta\xi_{MP}^{k+1} = B(x_{MP})\Delta u_i^{k+1} \quad (8)$$

Step 7. Update stresses using the constitutive model
Step 8. Update volume and density in material points using Eq. (9) and Eq. (10)

$$\Omega^{k+1}{}_{MP} = \Omega^{k}{}_{MP}\left(1 + \Delta\xi_{vol,MP}\right) \quad (9)$$

$$\rho^{k+1}{}_{MP} = \frac{\rho^{k}{}_{MP}}{1+\Delta\xi_{vol,MP}} \quad (10)$$

Step 9. Update the location of material points using Eq. (11)

$$x_{MP}^{k+1} = x_{MP}^{k} + \sum_{i=1}^{num,nod} N_i{}^{T}(\xi_{MP})\Delta u_i^{k+1} \quad (11)$$

Step 10. Bring back the computational mesh to its initial form, ignore nodal values, and carry out all material properties by material points.
In this paper, the soil media is considered as a completely dry sandy soil; therefore, single-phase simulation is sufficient to model the mechanical behavior of the soil mass. At step 7 of the described numerical algorithm, to calculate the stress vector (using Voigt notation), a constitutive relationship should be used. In this paper, the classical Mohr-Coulomb constitutive model (elastic-perfectly plastic model) is employed to determine the plastic behavior of the soil mass. However, there are some advanced constitutive models in the literature that can be applied to model the behavior of soils; it should be considered that the main aim of the paper is to evaluate the capabilities of the employed numerical approach (MPM) in the calculation of soil pressures on the retaining walls (not the adoption of advanced constitutive models in the MPM). The described algorithm is implemented in a MATLAB code to model the behavior of soil media in the paper.

2.2 Experimental tests

To evaluate the accuracy of the employed MPM models, two small-scale physical modeling tests are designed and performed. The main features of the used apparatus and applied tests are described in this section. Figure 2a shows the used apparatus, and Figure 2b demonstrates the schematic view and different parts of the apparatus. The desired motions of the wall can be applied using controllable step motors where the speed of the motors can be altered from 0.00125 to 0.25mm/s. To measure the observed wall motions, linear variable differential transformers (LVDT) are used. It should be mentioned that as the length of the model is large enough compared to its width (3 times), the behavior of soil mass can be considered as plane strain deformation. The movement of the wall in the first applied test is purely translational, while the movement in the second test is considered purely rotational.
In this study, Firoozkuh No. 161 moderate sand is employed as the soil material. The selected sandy soil is produced industrially by crushing parent rocks and contains particles with angular shapes. The main physical properties of the sand particles can be found in previously applied studies (for example, Tohidvand et al. [52 , 53]). The sand mechanical properties for the aimed relative density (Dr=60% for this study) are achieved using direct shear tests and reported in Table 1. The soil container was filled using the dry sand pluviation method to reach the considered relative density. To consider wall deformation as an active movement, wall deformation should be larger than 0.001H (H is the wall height). In this research, all tests contain at least 0.006H movement (Δx/H). Therefore, reaching the active stress condition of the soil is promising.

(a)

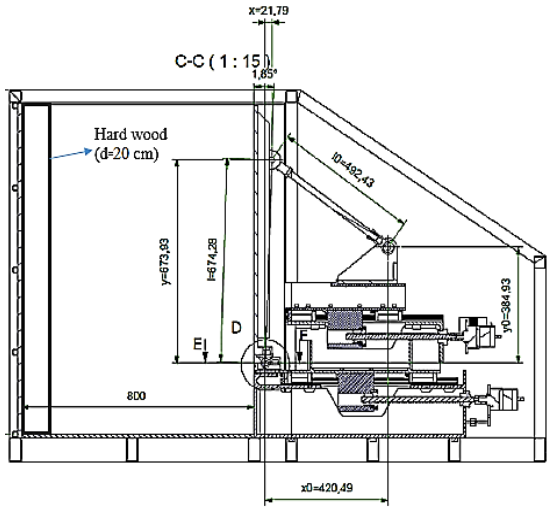

(b)

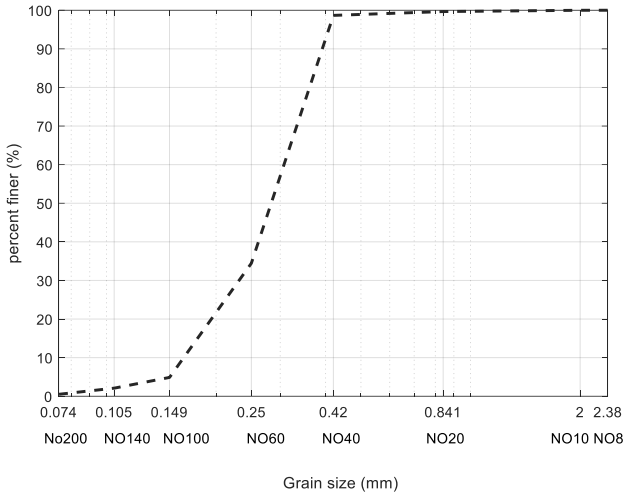

(c)

Fig. 2: (a) The employed apparatus for modeling the behavior of soils behind retaining walls (b) schematic view of the apparatus (c) grain size distribution of the used sand.

2.3 The used FEM model

In this paper, the second FEM model is employed to simulate the behavior of the soil behind the considered retaining walls, as well. The constitutive relations are modeled the same as the MPM by the classical Mohr-Coulomb constitutive model. Triangular six node-elements are used with a mesh that is shown in Figure 3. The rigid wall is modeled by beam elements in the FEM, while in the MPM, the rigid wall is modeled using volumetric elements.

3. Results

To evaluate the accuracy of the MPM in the calculation of the soil pressures on the retaining walls (by considering arching effects), two examples are considered. Both examples are modeled using small-scale physical modeling tests (as described in section 2.2), and then the results of the MPM are compared with the experimental results. Both experimental and numerical approaches employed small-scale physical modeling dimensions. However, in the 1g physical modeling tests, stresses are small, and these tests can only be scaled using geometrical scaling; as both experiments and the numerical method use the same dimensions, the results are comparable. The main issue would be the conversion of the model results to the prototype, while such a conversion was not applied in this research. In addition, the results of the MPM are compared with the previously proposed analytical approach by Khosravi et al. (2016) [54]. This analytical approach is selected because it has been calibrated with the same physical modeling tests employed in this paper. Both modeled retaining walls simulate an active deformation, where in the first example, the translational movement of the wall is modeled, and in the second example, the rotational movement is considered.

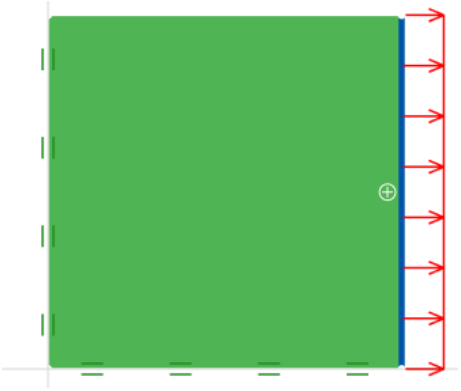

(a)

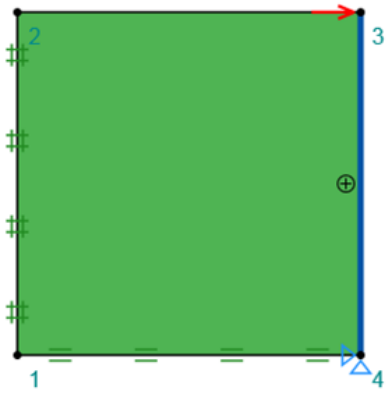

(b)

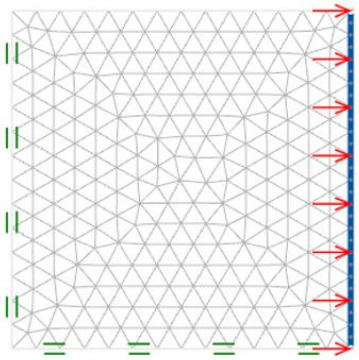

(c)

Fig. 3: (a) Considered model for translational movement (b) considered FEM model for rotational movement (c) a sample of employed meshes.

3.1 Retaining wall with translational movement

The translational movement of a rigid retaining wall is modeled using a simulation of a soil container with dimensions of 60m×60m, as shown in Figure 4. The rigid wall is modeled using volumetrical elements where the wall has 10cm of width and 60cm of depth. The base of the model is also modeled by volumetrical elements with a depth of 10cm and a length of 70cm. For translational movement, this base is considered rigid, the same as the wall. The rigidity of

the wall and base is ensured by selecting a high elastic modulus for them compared to the soil mass (10000 times larger). The selected material properties are detailed in Table 1. Four node 2D elements are used for computational mesh, and both active (filled with material points) and inactive elements (without any material point at the commencement of the analysis) are employed, as shown in Figure. 4. The achieved distribution of shear strains and normalized horizontal stresses are shown in Figure 5.

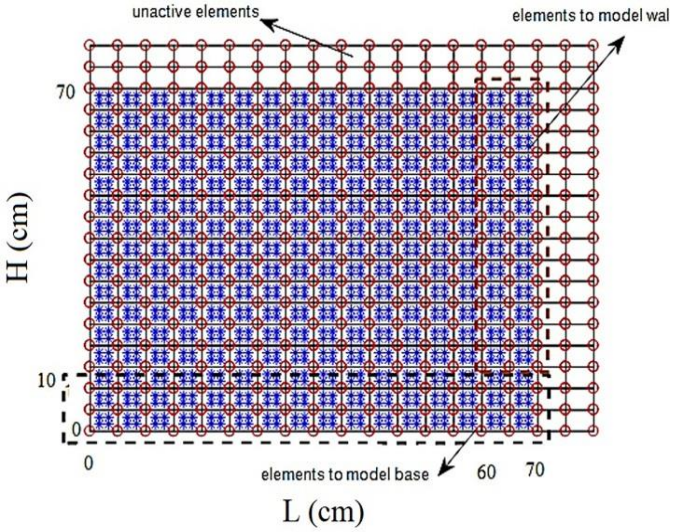

Fig. 4: MPM model for simulating the behavior of soil mass behind retaining wall.

The normalized horizontal stresses are compared with the results of the analytical method and the experimental test Figure 6. This figure shows that the employed MPM is capable of modeling arching effects as the resulting horizontal stresses decrease by approaching the bottom of the wall. In addition, the resultant horizontal force on the wall occurred higher than the 1/3H (H is the height of the wall) because of the arching effects.

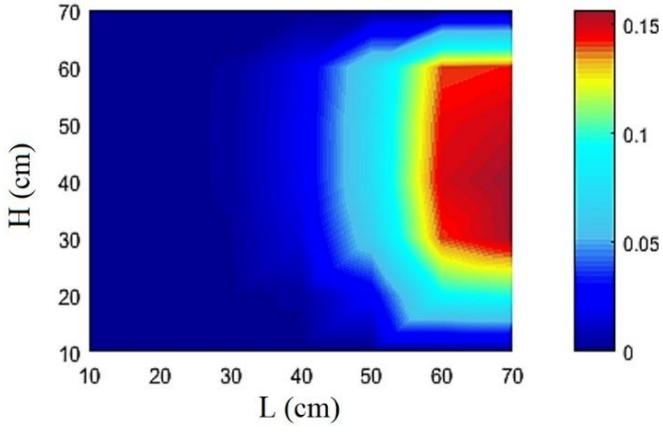

(a)

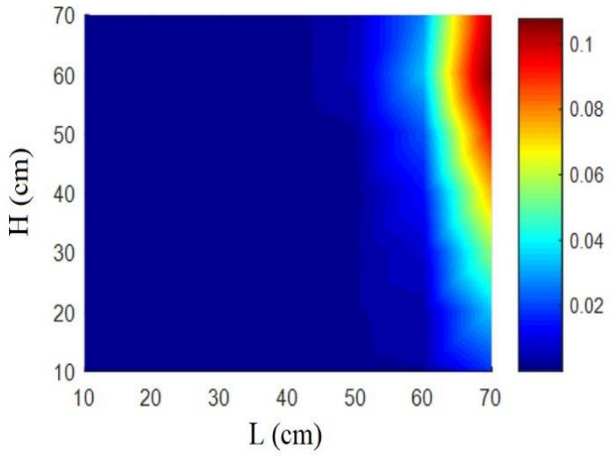

(b)

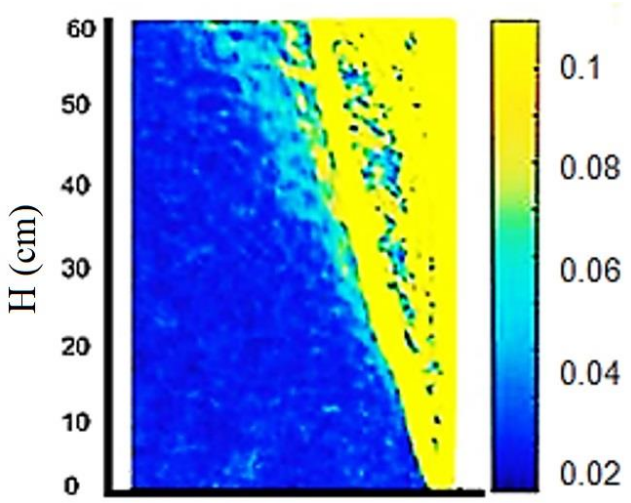

(c)

Fig. 5: Results of the MPM for rigid wall with translational movement (a) distribution of shear strains (b) distribution of normalized horizontal stresses ($\sigma_h/\gamma H$) (c) distribution of shear strains in the soil mass in the experimental test achieved by the PIV method.

The result of the FEM modeling is presented in Figure 7. Comparing the result of MPM and FEM (Figure 5 and Figure 7) shows that the FEM can model arching effects; however, the MPM method has better convergence to the analytical approach. Therefore, it can be stated that the MPM has more accuracy in the calculation of the active horizontal pressures on the retaining walls with translational movements. In Table 1, soil strength properties were achieved using direct shear tests, unit weight was determined by performing sand elevation on a mold (with known dimensions and volume) with different heights of elevation, and the stiffness properties (elastic modulus and Poisson's ratio were achieved using correlation relationships between soil relative density and these parameters.

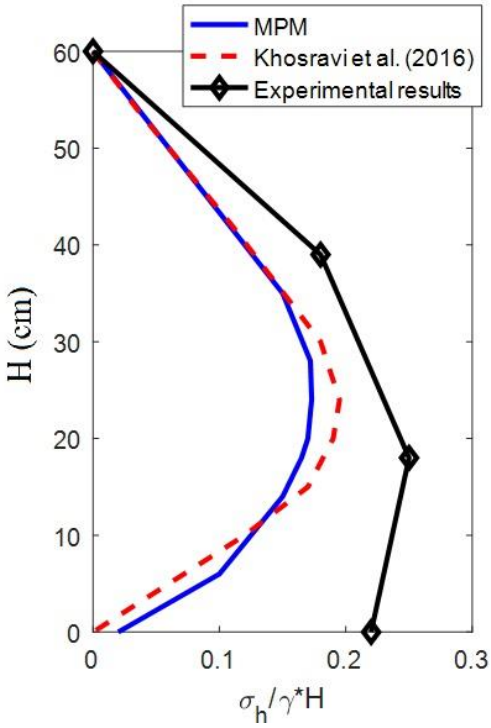

Fig. 6: Comparison between the results of the MPM with the analytical and experimental methods.

Table 1: Mechanical properties of the soil media

Unit weight (kN/m^3)	Elastic modulus (kN/m^2)	Cohesion (kN/m^2)	Friction angle	Poisson's ratio
16.8	24000	5	35	0.3

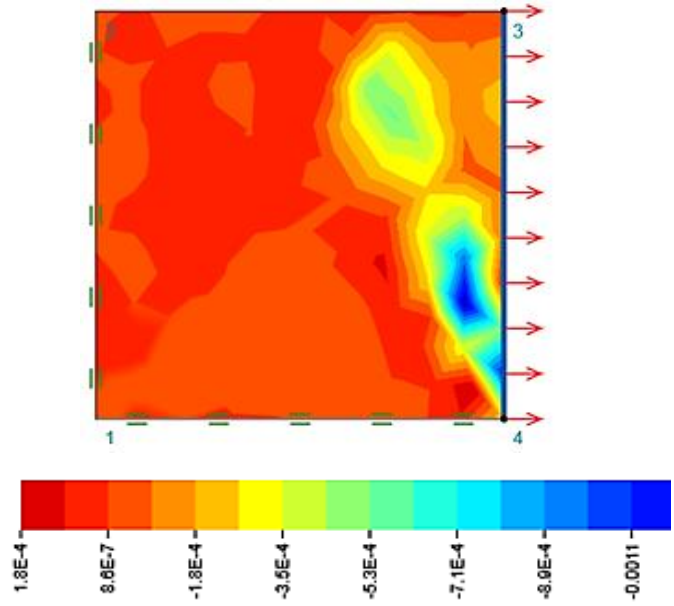

(a)

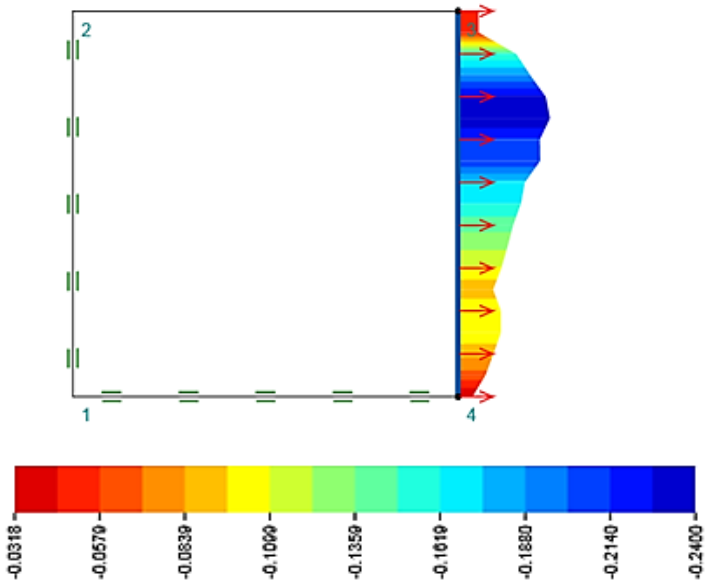

(b)

Fig. 7: Results of the FEM (a) distribution of shear strains (b) normalized horizontal pressure on the wall.

3.2 Retaining wall with rotational movement

In this section, the active rotational movement of a rigid retaining wall is modeled using the MPM. The model has the same dimensions as described in section 3.1. Therefore, the same computational mesh is used. The rotation is considered about the outer edge (point A in Figure 8) of the base of the wall. Material properties of the soil mass are the same as detailed in Table 1. The resulting distribution of shear strains and normalized horizontal stresses are shown in Figure 9. As the figure shows, the employed MPM efficiently modeled the effects of arching, where the location of the resultant force and distribution of the pressures on the wall are different from the ones proposed by classical Rankine theory.

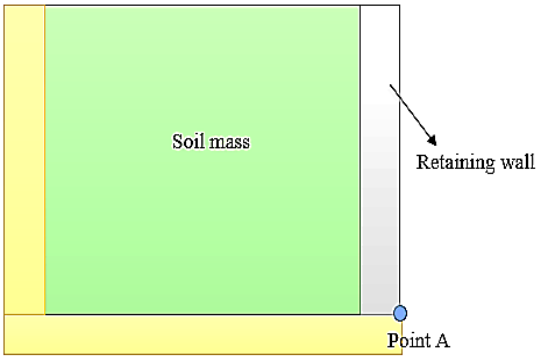

Fig. 8: Considered model for rotational movement of the rigid wall.

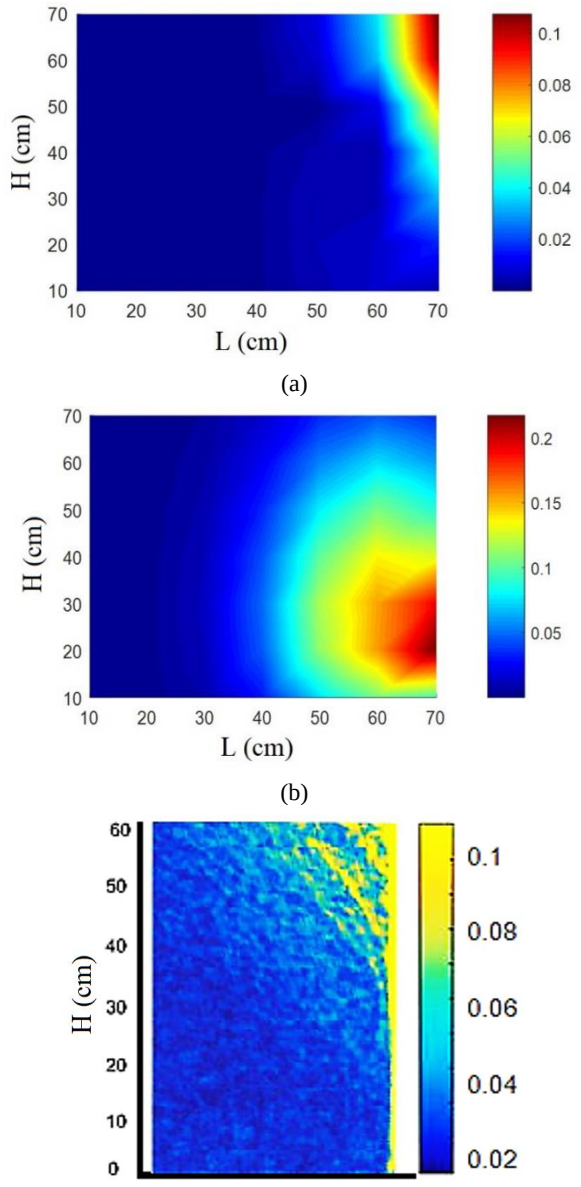

Fig. 9: Results of the MPM for rigid wall with rotational movement (a) distribution of shear strains (b) distribution of normalized horizontal stresses ($\sigma_h/\gamma H$) (c) distribution of shear strains in the soil mass in the experimental test achieved by the PIV method.

A comparison between the resulting normalized horizontal stresses on the wall with the experimental and the FEM is presented in Figures 11 and 12, respectively. As Figure 9 and Figure 10 show, the results of the MPM have a good agreement for shear strain distribution and less convergence in the horizontal pressures compared to the experimental results.

Figure 11 demonstrates the FEM is not capable of accurately simulating pressures on the retaining wall for rotational movement of the wall. Therefore, it can be stated that the MPM can model arching effects for rigid retaining walls with active rotational movements compared to FEM.

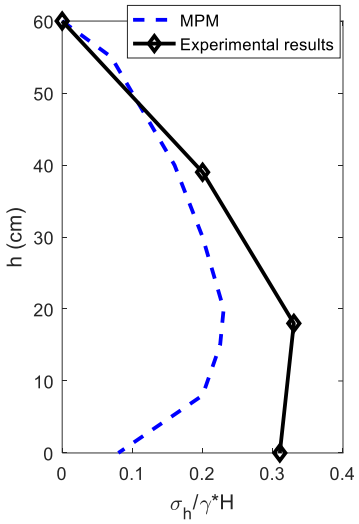

Fig. 10: Comparison between the results of the MPM with the experimental test.

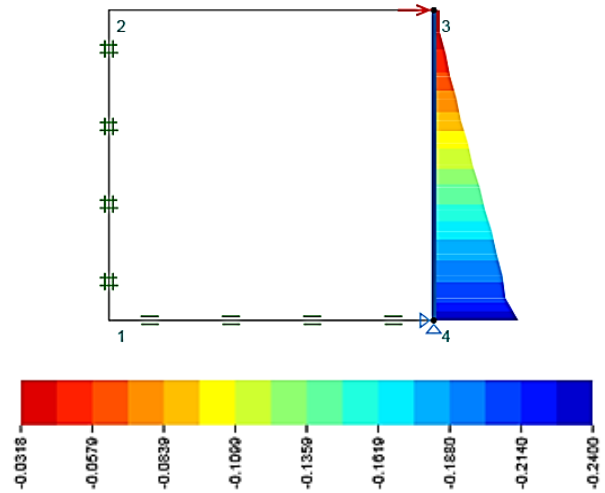

Fig. 11: Results of the FEM (a) distribution of shear strains (b) normalized horizontal pressure on the wall.

4. Conclusion

In this paper, the accuracy of the material point method in the simulation of the behavior of soil media behind retaining walls is evaluated for the first time in the literature. To this aim, active translational and rotational movements of a rigid retaining wall are considered. The retaining wall is modeled using the small-scale physical modeling approach and finite element method as well. The comparison between the results indicates that the MPM is capable of modeling arching effects in the soil media more accurately than the FEM. However, the results of the MPM in the calculation of the lateral pressures are smaller than the experimental results, but well agreements are achieved compared to the analytical approach for translational movement of the wall. For rotational movement, the deviation from experimental results is larger for lateral pressures; however, shear strain distributions are in good agreement. The achieved results indicate that, however, the MPM can model arching effects in the soil mass for both translational and rotational movements; the FEM cannot model arching effects for rotational movement of the wall accurately.

References

[1] Terzaghi, Karl. Theoretical soil mechanics. John Wiley & sons New York (1943): 11-15.

[2] Patel, S., & Deb, K. (2020). Study of active earth pressure behind a vertical retaining wall subjected to rotation about the base. International Journal of Geomechanics, 20(4), 04020028.

[3] Abbasnezhad, A., and Sadr, Karimi, J. (2008). An experimental investigation into the arching effect in fine sand.

[4] Li, Z. W., & Yang, X. L. (2018). Active earth pressure for soils with tension cracks under steady unsaturated flow conditions. Canadian Geotechnical Journal, 55(12), 1850-1859.

[5] Zhang, H., Chen, J., & Xu, M. (2022). The Determination of Rational Spacing of Anti-Slide Piles and Soil Pressure on Pile Sheet Based on Soil Arching Effect. Geotechnical and Geological Engineering, 40(5), 2857-2866.

[6] Janssen, H. A. (1895). Versuche uber getreidedruck in silozellen. Z. ver. deut. Ing., 39, 1045.

[7] Frydman, S., & Keissar, I. (1987). Earth pressure on retaining walls near rock faces. Journal of Geotechnical Engineering, 113(6), 586-599.

[8] Chenghua, W., Yongbo, C., & Lixiang, L. (2001). Soil arch mechanical character and suitable space between one another anti-sliding pile. Journal of Mountain Science, 19(6), 556-559.

[9] Paik, K. H., & Salgado, R. (2003). Estimation of active earth pressure against rigid retaining walls considering arching effects. Geotechnique, 53(7), 643-653.

[10] Spangler, M. G., & Handy, R. L. (1973). Soil engineering (No. 624.151 S6 1973).

[11] Goel, S., & Patra, N. R. (2008). Effect of arching on active earth pressure for rigid retaining walls considering translation mode. International Journal of Geomechanics, 8(2), 123-133.

[12] Pipatpongsa, T., & Heng, S. (2010). Granular arch shapes in storage silo determined by quasi-static analysis under uniform vertical pressure. Journal of Solid Mechanics and Materials Engineering, 4(8), 1237-1248.

[13] Dalvi, R. S., & Pise, P. J. (2012). Analysis of arching in soil-passive state. Indian Geotechnical Journal, 42(2), 106-112.

[14] Bahmani Tajani, S., Fathipour, H., Payan, M., Jamshidi Chenari, R., & Senetakis, K. (2022). Temperature-dependent lateral earth pressures in partially saturated backfills. European Journal of Environmental and Civil Engineering, 1-27.

[15] Deng, B., & Yang, M. (2019). Analysis of Passive Earth Pressure for Unsaturated Retaining Structures. International Journal of Geomechanics, 19(12), 06019016.

[16] Fathipour, H., Tajani, S. B., Payan, M., Chenari, R. J., & Senetakis, K. (2022). Influence of transient flow during infiltration and isotropic/anisotropic matric suction on the passive/active lateral earth pressures of partially saturated soils. Engineering Geology, 310, 106883.

[17] Fathipour, H., Payan, M., & Chenari, R. J. (2021). Limit analysis of lateral earth pressure on geosynthetic-reinforced retaining structures using finite element and second-order cone programming. Computers and Geotechnics, 134, 104119.

[18] Shahrokhabadi, S., Vahedifard, F., Ghazanfari, E., & Foroutan, M. (2019). Earth pressure profiles in unsaturated soils under transient flow. Engineering Geology, 260, 105218.

[19] Liang, W. B., Zhao, J. H., Li, Y., Zhang, C. G., & Wang, S. (2012). Unified solution of Coulomb's active earth pressure for unsaturated soils without crack. In Applied Mechanics and Materials (Vol. 170, pp. 755-761). Trans Tech Publications.

[20] Stanier, S., & Tarantino, A. (2010). Active earth force in 'cohesionless' unsaturated soils using bound theorems of plasticity. In Proc. of 5th Int. conf. on Unsaturated Soils, Barcelona (pp. 1081-1086).

[21] Sahoo, J. P., & Ganesh, R. (2017). Active Earth Pressure on Retaining Walls with Unsaturated Soil Backfill. In International Congress and Exhibition" Sustainable Civil Infrastructures: Innovative Infrastructure Geotechnology" (pp. 1-19). Springer, Cham.

[22] Pufahl, D. E., Fredlund, D. G., & Rahardjo, H. (1983). Lateral earth pressures in expansive clay soils. Canadian Geotechnical Journal, 20(2), 228-241.

[23] Veiskarami, M., Chenari, R. J., & Jameei, A. A. (2019). A study on the static and seismic earth pressure problems in anisotropic granular media. Geotechnical and Geological Engineering, 37(3), 1987-2005.

[24] Mirmoazen, S. M., Lajevardi, S. H., Mirhosseini, S. M., Payan, M., & Jamshidi Chenari, R. (2022). Limit analysis of lateral earth pressure on geosynthetic-reinforced retaining structures subjected to strip footing loading using finite element and second-order cone programming. Iranian Journal of Science and Technology, Transactions of Civil Engineering, 46(4), 3181-3192.

[25] Payan, M., Fathipour, H., Hosseini, M., Chenari, R. J., & Shiau, J. S. (2022). Lower Bound Finite Element Limit Analysis of Geo-Structures with Non-Associated Flow Rule. Computers and Geotechnics, 147, 104803.

[26] Mirmoazen, S. M., Lajevardi, S. H., Mirhosseini, S. M., Payan, M., & Chenari, R. J. (2021). Active lateral earth pressure of geosynthetic-reinforced retaining walls with inherently anisotropic frictional backfills subjected to strip footing loading. Computers and Geotechnics, 137, 104302.

[27] Vahedifard, F., Leshchinsky, B. A., Mortezaei, K., & Lu, N. (2015). Active earth pressures for unsaturated retaining structures. Journal of Geotechnical and Geoenvironmental Engineering, 141(11), 04015048.

[28] Patki, M. A., Mandal, J. N., & Dewaikar, D. M. (2015). Determination of passive earth pressure coefficients using limit equilibrium approach coupled with the Kötter equation. Canadian Geotechnical Journal, 52(9), 1241-1254.

[29] Vo, T., & Russell, A. R. (2014). Slip line theory applied to a retaining wall–unsaturated soil interaction problem. Computers and Geotechnics, 55, 416-428.

[30] Zhang, C. G., Zhu, D. H., Gao, Z., Xue, G. W., & Li, Z. (2012). Unified Solution of Passive Earth Pressure for Unsaturated Soils. In Advanced Materials Research (Vol. 594, pp. 430-433). Trans Tech Publications.

[31] Farajniya, R., Poursorkhabi, R. V., Zarean, A., & Dabiri, R. (2022). Investigation of the arching in rock-fill dam ten years after end construction using Numerical analysis and monitoring. Ferdowsi Civil Engineering, 35(1), 59-74.

[32] Zhao, L. H., Luo, Q., Li, L., Yang, F., & Yang, X. L. (2009). The upper bound calculation of passive earth pressure is based on the shear strength theory of unsaturated soil. In Slope Stability, Retaining Walls, and Foundations: Selected Papers from the 2009 GeoHunan International Conference (pp. 151-157).

[33] Soubra, A. H. (2000). Static and seismic passive earth pressure coefficients on rigid retaining structures. Canadian Geotechnical Journal, 37(2), 463-478.

[34] Fathipour, H., Siahmazgi, A. S., Payan, M., & Chenari, R. J. (2020). Evaluation of the lateral earth pressure in unsaturated soils with finite element limit analysis using second-order cone programming. Computers and Geotechnics, 125, 103587.

[35] Fathipour, H., Payan, M., Jamshidi Chenari, R., & Senetakis, K. (2021). Lower bound analysis of modified pseudo-dynamic lateral earth pressures for retaining wall-backfill system with depth-varying damping using FEM-Second order cone programming. International Journal for Numerical and Analytical Methods in Geomechanics, 45(16), 2371-2387.

[36] Li, X., Wu, Y., & He, S. (2010). Seismic stability analysis of gravity retaining walls. Soil Dynamics and Earthquake Engineering, 30(10), 875-878.

[37] Subba Rao, K. S., & Choudhury, D. (2005). Seismic passive earth pressures in soils. Journal of Geotechnical and Geoenvironmental Engineering, 131(1), 131-135.

[38] Aalami, M. T., Vafaeipoor, R., Naseri, A., & Mojtahedi, A. (2022). Experimental Analysis of the Effect of the Distance of a Submerged Berm in front of a Reshaping Rubble Mound Breakwater on Diminishing the Damage Parameter. Journal of Civil and Environmental Engineering, 52(107), 1-13.

[39] Nakai, T. (1985). Analysis of earth pressure problems considering the influence of wall friction and wall deflection. In International conference on numerical methods in geomechanics (pp. 765-772).

[40] Dasgupta, U. S., Chauhan, V. B., & Dasaka, S. M. (2017). Influence of spatially random soil on lateral thrust and failure surface in earth retaining walls. Georisk: Assessment and Management of Risk for Engineered Systems and Geohazards, 11(3), 247-256.

[41] Hajialilue-Bonab, M., & Tohidvand, H. R. (2015). A modified scaled boundary approach in frequency domain with diagonal coefficient matrices. Engineering Analysis with Boundary Elements, 50, 8-18.

[42] Hassanzadeh, M., Tohidvand, H. R., Hajialilue-Bonab, M., & Javadi, A. A. (2018). Scaled boundary point interpolation method for seismic soil-tunnel interaction analysis. Computers and Geotechnics, 101, 208-216.

[43] Morgun, A., & Balatiuk, A. (2013). STABILITY OF RETAINING WALLS BY BEM. Scientific Works of Vinnytsia National Technical University, (2).

[44] Harlow, F. H. (1964). The particle-in-cell computing method for fluid dynamics. Methods Comput. Phys., 3, 319-343.

[45] Sulsky, D., Chen, Z., & Schreyer, H. L. (1994). A particle method for history-dependent materials. Computer methods in applied mechanics and engineering, 118(1-2), 179-196.

[46] Higo, Y., Lee, C. W., Doi, T., Kinugawa, T., Kimura, M., Kimoto, S., & Oka, F. (2015). Study of dynamic stability of unsaturated embankments with different water contents by centrifugal model tests. Soils and Foundations, 55(1), 112-126.

[47] Wang, F., Li, X., Couples, G., Shi, J., Zhang, J., Tepinhi, Y., & Wu, L. (2015). Stress arching effect on stress sensitivity of permeability and gas well production in Sulige gas field. Journal of Petroleum Science and Engineering, 125, 234-246.

[48] Ceccato, F., Beuth, L., Vermeer, P. A., & Simonini, P. (2016). Two-phase material point method applied to the study of cone penetration. Computers and Geotechnics, 80, 440-452.

[49] Bolognin, M., Martinelli, M., Bakker, K. J., & Jonkman, S. N. (2017). Validation of material point method for soil fluidization analysis. Journal of Hydrodynamics, Ser. B, 29(3), 431-437.

[50] Kiriyama, T., Fukutake, K., & Higo, Y. (2018). Verification and validation of two-phase material point method simulation of pore water pressure rise and dissipation in earthquakes. In Physical Modelling in Geotechnics (pp. 215-220). CRC Press.

[51] Giridharan, S., Gowda, S., Stolle, D. F., & Moormann, C. (2020). Comparison of ubcsand and hypoplastic soil model predictions using the material point method. Soils and Foundations, 60(4), 989-1000.

[52] Tohidvand, H. R., Hajialilue-Bonab, M., Katebi, H., Nikvand, V., & Ebrahimi-Asl, M. (2022). Monotonic and post cyclic behavior of sands under different strain paths in direct simple shear tests. Engineering Geology, 302, 106639.

[53] Tohidvand, H. R., Hajialilue-Bonab, M., & Katebi, H. (2024). Evaluation of the Effects of Different Strain Paths on the Behavior of Sands Using Direct Simple Shear Tests. Journal of Testing and Evaluation, 52(1).

[54] Khosravi, M. H., Takemura, J., Pipatpongsa, T., & Amini, M. (2016). In-flight excavation of slopes with potential failure planes. Journal of Geotechnical and Geoenvironmental Engineering, 142(5), 06016001.